SCIREA Journal of Materials Science

http://www.scirea.org/journal/Materials

October 17, 201

Volume 1, Issue1, October 2016

Numerical Modeling of Microstructure of Heat Affected Zone in Friction Stir Welded AA7075

A. Abdollah-zadeh[1], A. Mehri, S. Entesari, H. Assadi

Tarbiat Modares University, Department of Materials Engineering, P.O. Box: 14115-143, Tehran, Iran

[1] Corresponding author: zadeh@modare.ac.ir

Abstract

There is interest in the study and control of heat affected zone (HAZ) of the weld junctions, which is often regarded as the weakest point of the joints. In the present work, experimental and numerical analyses are used to characterize extension and microstructure of HAZ in friction stir welding (FSW) of 7075 Al alloy (AA) sheets. The thermal history was recorded by inserting thermocouples near the HAZ. These measurements were combined with a numerical modeling to predict thermal histories of various welding conditions. Moreover, the grain growth behavior of the base metal, including the growth kinetic constant, was determined through a series of isothermal annealing at different temperatures followed by grain size measurements. In this way, the grain structure of the HAZ could be linked to the welding conditions. A good agreement between the predicted and observed values was obtained over a wide range of conditions.

Keywords: AA7075; HAZ; Numerical modeling; Thermal cycle, FSW

1. Introduction

Friction stir welding (FSW) introduced by TWI in 1991, is considered a break though in the welding of heat-treatable aluminum alloys that are generally considered as non-weldable alloys [1]. In this method, a rotating non-consumable tool, including a shoulder and penetrating pin, is moving along the two parts. Pin movement and rotation makes a stirred zone with fine-fully recrystallized structure. Thermo-mechanically affected zone (TMAZ) surrounding the nugget zone contains plastically deformed grains and experienced the high heat flux of the welding. The ending part of the weldment located between the TMAZ and base metal is HAZ.

The HAZ of the welded junctions are often the weakest point of the joints [2]. So, studies on the characterization and developing the knowledge of this region could be counted essential in process optimizations. Process parameters of the welding and physical properties of the joints are the most effective parameters on the microstructure and extension of HAZ which make the prediction about its attributes to be sophisticated. Thus, developing a model for HAZ would be so valuable. The simulation of HAZ has been previously carried out by some workers [3,4]. However, no validated work has been reported yet on the simulation and prediction of the HAZ in FSW joints. So, lack of a model for prediction the structure of the HAZ of FSW joints was a motivation force for this research.

In this work, thermal cycles of FSW were recorded using insertion of thermocouples on the 7075-T6 Al alloy. Then, grain growth kinetic parameter of the base metal was obtained using the isothermal annealing. The classic formula for Grain growth is as follows [5]:

$$D^2 - D_0^2 = K_o \exp(-Q/RT)\, t \qquad \textbf{(1)}$$

in which *D, D₀, K₀, Q, R, T* and *t* are mean final grain size, original grain size, material constant, activation energy of grain growth, gasses universal constant, absolute temperature and time, respectively. For calculation of the grain growth of the transient thermal cycle, the modified form of that is derived as:

$$D^2 - D_0^2 = K_o \int_{t_1}^{t_2} \exp(-Q/RT(t))\, dt \qquad \textbf{(2)}$$

This formulation can be used to couple the thermal cycle and grain growth occurred in the HAZ [6,7]. So, using grain growth parameters, a numerical calculation of the amount of grain growth occurred in the HAZ due to experienced thermal cycle would be possible. This model would enable us for prediction of the HAZ microstructure and also coupling the thermal cycle information to microstructural features. Moreover, the HAZ microstructure could be predicted for different welding conditions. Simulation outputs were validated by experimental results. On the other hand, as the end of the HAZ is not usually distinguished clearly, using the developed model, a criteria would be laid down to overcome this problem.

2. Materials and Methods

Two 300×5×1.2mm thin sheets of Aluminum alloy of 7075-T6 were joined to each other using FSW. Chemical composition of the material is brought in Table 1. Two sheets were clamped to the FSW machine anvil firmly with the rolling direction perpendicular to welding direction. Fig. 1 shows the welding setup and the FSW tool. The tool dimensions employed here are summarized in the Table 2.

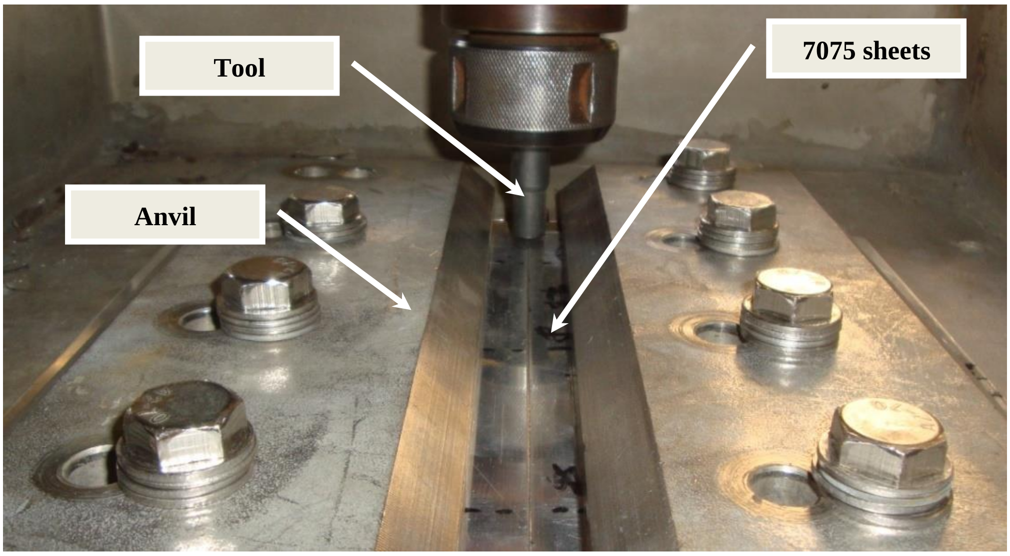

Fig. 1. FSW setup demonstrating the two Al sheets clamped to the anvil of the FSW machine.

Table 1. Chemical composition of the 7075-T6 Aluminum alloy in wt%.

Al	Si	Fe	Ti	Mg	Cu	Zn
balance	0.020	0.034	0.038	2.37	1.91	5.86

Table 2. FSW tool dimensions in mm.

Pin diameter	Shoulder diameter	Pin height
3	12	1.1

Sufficient precious thermocouples inserted into the specimens in order to record thermal cycles of the welding thorough FSW route. They were completely joined to the samples and then accurately calibrated in the error range as low as $\pm 3^{\circ}\mathrm{C}$. The configuration of the thermocouples is schematically exhibited in the Fig. 2. The first thermocouple was stacked to the sample just a millimeter aside of the welding zone to observe the hottest HAZ temperature.

Welding procedure was done by welding speed (V) of 50 mm/min and stirring rotational speed (ω) of 800 and 1000 rpm. The Keller's agent was used for chemical etching. The mean grain size was measured by linear intercept method of the area under the inserted thermocouples.

Using the method of Feltham [8], grain growth parameters of 7075-T6 Al alloy thin sheets were experimentally extracted in order to simulate the effect of the welding thermal cycles on the grain growth of the FSW in HAZ. According to this method, several samples of the alloy were isothermally annealed for different time. Subsequently, the mean grain size was measured by Optical Microscopy (OM). The times and temperatures of isothermal annealing are summarized in Table 3.

Table 3. The temperatures and times of isothermal annealing.

Temperature (K)	Time (min.)
493	30
	60
	120
593	32
	120
693	30
	60
	140
753	30
	60

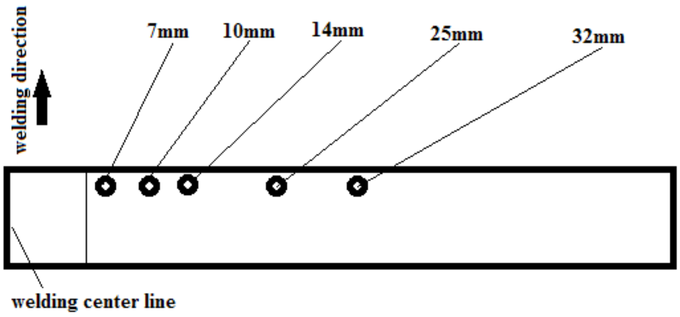

Fig. 2. Configuration of the thermocouples for recording the temperature-time cycle during FSW.

3. Results

Fig. 3 exhibits the values of D^2 versus time obtained from fitting the Equation 1 on the grain growth data of 7075-T6 Al alloy due to isothermal annealing. It confirms the applicability of the equation in this case.

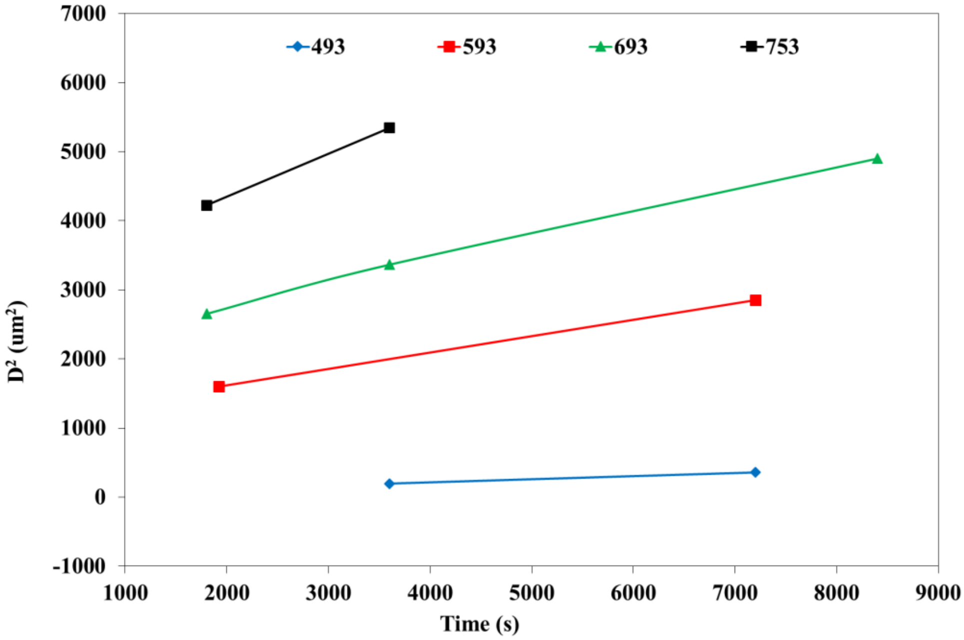

Fig. 3. Application of Equation 1 on the isothermal annealing of aluminum 7075-T6 Al alloy.

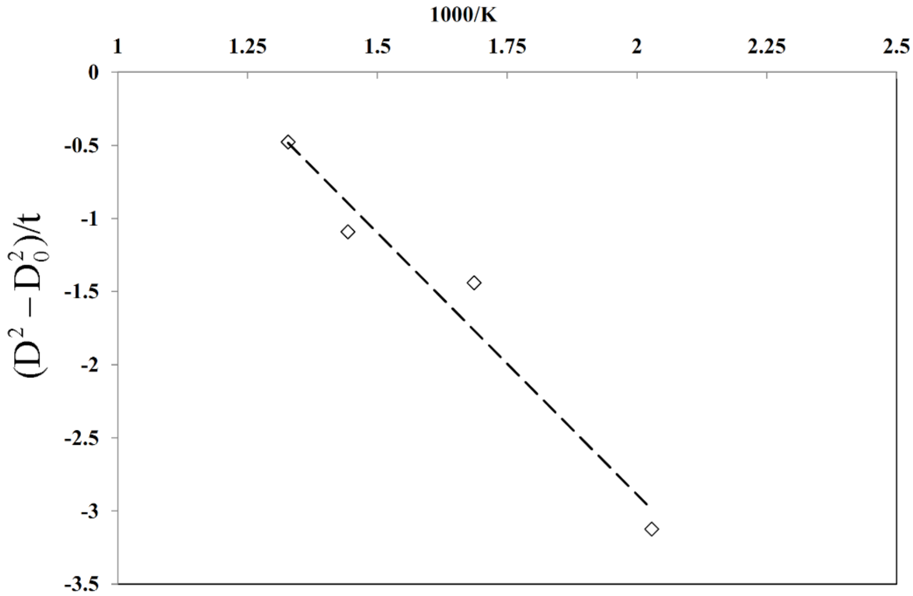

Fig. 4. $(D^2-D_0^2)/t$ **vs.** $1/T$ **for isotherms of Fig. 3.**

The slops of the isotherms of Fig. 3 versus T^{-1} are exhibited in Fig. 4. The straight line could also be figured out on the Fig. 4. Herein, kinematic parameter of grain growth of the alloy can be calculated as follow. Assumed the line formula is:

$$Y = aX + b \qquad (3)$$

Then

$$\log(K_o) = b$$

The slope of the line is:

$$-Q/R = a$$

Then

$$K_o = 71.45\,\mu m^2 S^{-1}$$

And

$$-Q/R = -3578$$

So, the activation energy of grain growth is resulted as:

$$Q = 29747.49 \text{ j/mol}$$

Using the values of grain growth kinetic parameters, the effect of the FSW thermal cycle on the HAZ grain growth can be calculated. Fig. 5 and 6 show the thermal temperature-time diagrams of the welding process by experimental endeavors. It is reasonable that with increasing the distance from the welding center line, the peak temperatures of the diagrams are declined.

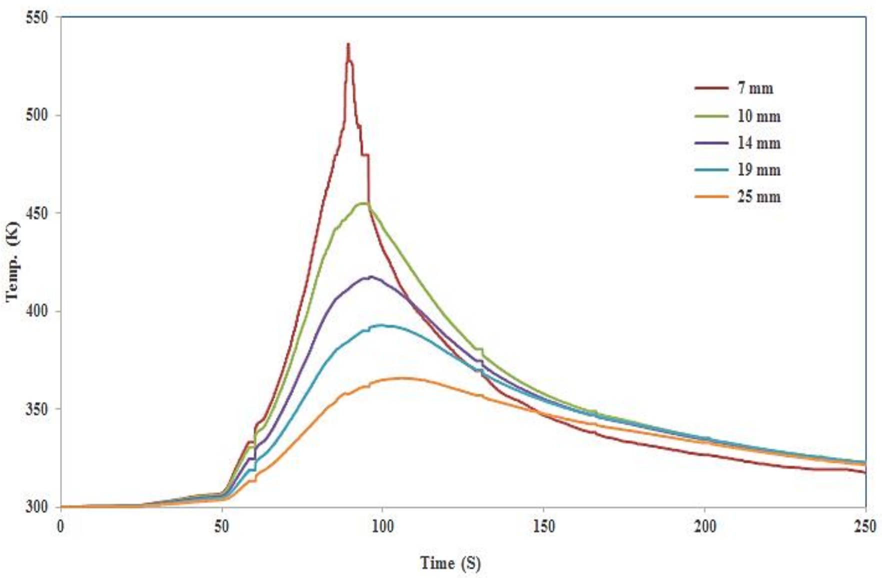

Fig. 5. Temperature-Time diagrams for different distances from welding center line for the sample prepared by V=50mm/min and ω=800 rpm.

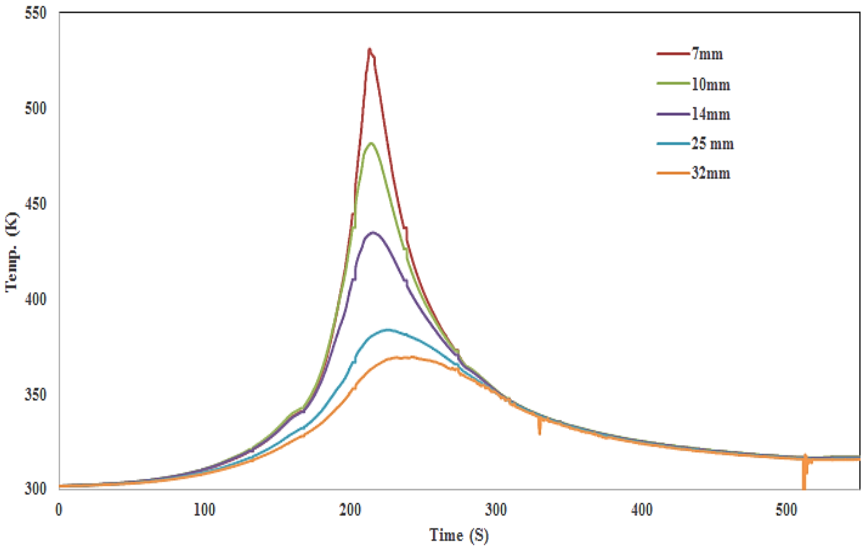

Fig. 6. Temperature-Time diagrams for different distances from welding center line for the sample prepared by V=50mm/min and ω=1000 rpm.

Integration of the Equation 2 can be calculated by forward step-wise summing on each temperature-time diagram as:

Integration of the equation 2 can be calculated by forward step-wise summing on each temperature-time diagram. In this method, thermal cycle is divided on finite time increments and grain growth in each step is calculated. Finally, all of them are summed up as Equation 4 and grain growth for the thermal cycle can be calculated.

$$D^n - D^n = k_o \sum_i \exp(-Q / RT_{i-1}).\Delta t_i \qquad (4)$$

in which i and Δt are standing for each step of temperature-time number and time span, respectively. The Δt in this study were hold in experiments at constant value of 0.02 S. Calculated mean grain size for each thermal cycle curve by equation 3 are summarized in Table 4. The base metal mean grain size is measured about 33 μm. Fig. 7 and 8 show the microstructure of the HAZ prepared by OM. Which cover a distance between 6 to 15mm from welding centerline. Equiaxed fined grained of welding nugget zone can be seen in the left-down corner of the pictures. The mean grain size in the HAZ monotonously decreases from the maximum size toward the base metal grain size.

Table 4. Mean grain size of HAZ for different distances from welding centerline of FSW (ω=800 and 1000 rpm, V=50mm/min) calculated for recorded thermal cycles, respectively.

Distance from welding center line (mm)	Mean grain size (μm)	
	800 rpm	**1000 rpm**
7	52.1	73.0
10	48.6	62.8
14	43.3	53.0
19	40.8	-
25	38.4	45.3
32	-	43.5

Fig. 7. Panoramic picture of the HAZ of the FS Welded sample of 800 rpm-50mm/min.

Fig. 8. Panoramic picture of the HAZ of the FS Welded sample of 1000 rpm-50mm/min.

Figs. 9 and 10 are indicating reasonable agreement between the predicted and observed values of grain size of HAZ. It means that the present method can be useful with acceptable results.

The extension of the HAZ is the other parameters that can be found by this model, either. If the end of the HAZ be roughly considered as a place where the mean grain size growth is less than 10% of that of the base metal, by extrapolation of the diagram of Fig. 9, the end of the HAZ can be proposed to be about 50mm from the centerline.

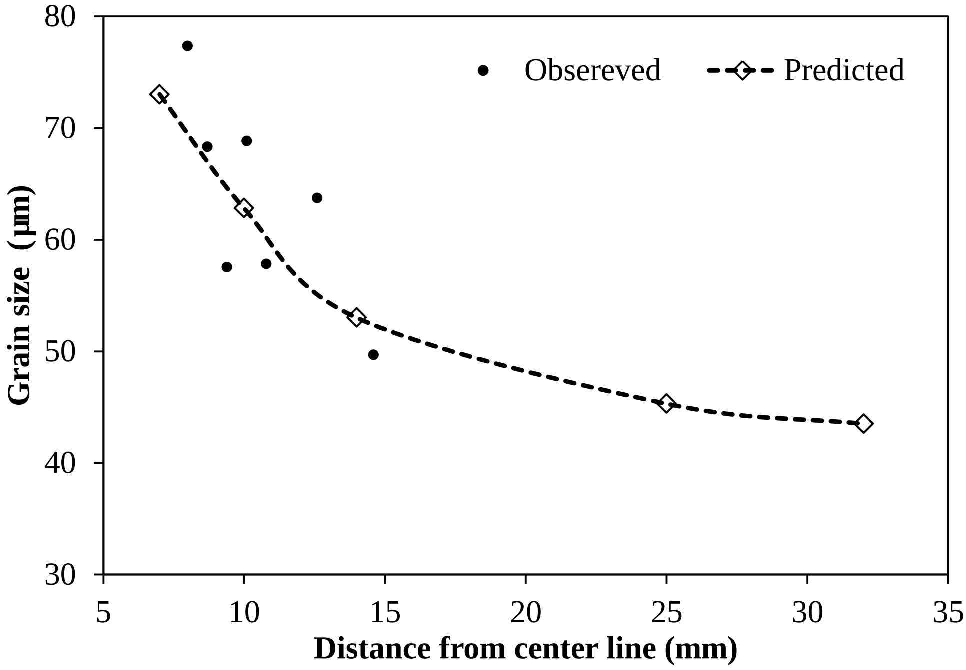

Fig. 9. Comparison of HAZ grain sizes from the predicted and observed values of FSW (1000 rpm, 50mm/min).

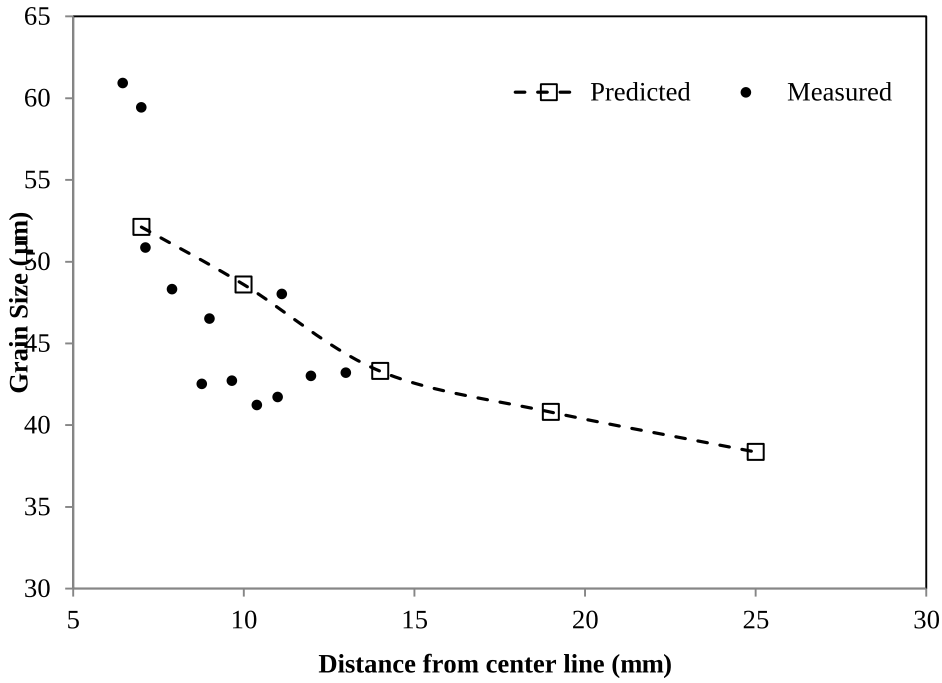

Fig. 9. Comparison of HAZ grain sizes from the predicted and observed values of FSW (1000rpm, 50mm/min).

4. Conclusions

A simple numerical model is proposed to predict the effect of the thermal cycles of FSW on the microstructure of the HAZ. It could be validated due to the good agreements of the calculated values and the real experimental data. So, this model can be employed for a wide range of the experimental conditions of welding that higher time and cost consumptions can be highly impeded.

5. References

[1] R. S. Mishra, M. W. Mahoney, "Friction stir welding and processing", ASM International, Ohio, 2007, p.3.

[2] G. Matters,"The welding of aluminum and its alloys", CRC press, North America, 2002, p. 13.

[3] H. Jamshidi Aval, S. Serajzadeh, A.H. Kokabi, "Prediction of grain growth behavior in HAZ during gas tungsten arc welding of 304 stainless steel", Materials Engineering and Performance, Vol. 18, 2009, pp. 1193–1200.

[4] M. Shome, "Effect of heat-input on austenite grain size in the heat-affected zone of HSLA-100 steel", Materials Science and Engineering A, 2007, Vol. 445–446, pp. 454–460.

[5] R. E. Reed-Hill, "Physical Metallurgy Principles", D Van Nostrand Company pulications, North America,1973, pp. 298-309.

[6] M. Shome , O.P. Gupta, O.N. Mohanty, "A modified analytical approach for modelling grain growth in the coarse grain HAZ of HSLA steels", Scripta Materialia, 2004, Vol. 50, pp. 1007–1010.

[7] H. Ikawa, S. Shin, H. Oshige, "Grain growth of commercial-purity nickel in welh-heat affected zone", Japan welding society, 1975, Vol. 6, pp.17-22.

[8] P. Feltham, G. J. Copley, "Grain growth in a-brasses", Acta Metallurgica, 1958, Vol. 6, pp. 539-543.